Dynamic Response of Wind Turbines taking into account the Rotational Component of Ground Motions

L. Hermanns, L.E. Quiros, J. Gaspar-Escribano & B. Benito
Universidad Politecnica de Madrid,Spain

M.A. Santoyo
Universidad Complutense de Madrid, Spain

J. Vega
CEMIM-F2I2, Madrid, Spain

SUMMARY:
This work studies the dynamic response of a wind turbine structure under seismic loading, taking into account the rotational component of ground shaking. The study covers both the definition of synthetic input ground motion, and the analysis of the dynamic response. Based on previous studies, carried out in the framework of a research project, and the common seismological characteristics of shallow earthquakes, the synthetic seismograms were generated using an appropriate set of source properties (e.g. focal mechanism, source time function, etc...) and an earth subsurface velocity structure for the region, taking into account the tectonic environment of the modelling site. Synthetic time histories have been computed using the Discrete Wavenumber Method, assuming a point source and a horizontal layered earth structure.

Results will be analyzed in order to assess the factors that lead to scenarios in which the contribution of the rotational components to the overall response cannot be neglected.

Keywords: Rotational component, Wind Turbine, Discrete Wavenunber Method

1. INTRODUCTION

Rotational ground motion analysis is a novel discipline of seismology that still presents significant unexplored fields. Accordingly, the development of instruments for recording rotational motions is limited. Thus, strong motion networks do not routinely measure these parameters. In this paper a set of complete synthetic ground motion time histories (i. e., including both translational and rotational components) was used in order to evaluate the seismic response of a wind turbine. This structure is interesting because it presents a large inertial mass at the top and a rotating component around a horizontal axis. Different methods to calculate the dynamic response of the structure are examined. At this stage of the analysis, a Finite Element model seems a good choice for performing transient dynamic calculations. The structural response of the wind turbine is characterized by the maximum value of Von Mises stress at different levels of the tower. The target turbine site corresponds to a hypothetic site located at Madrid Region (Spain), where moderate events could take place. Values of the corresponding seismological parameters are selected accordingly. However, the upper soil layer of the Earth velocity model is very stiff. This should always be remembered when interpreting the results.

2. SEISMICITY AND SEISMIC HAZARD IN CENTRAL SPAIN

Central Spain is characterized by a relatively low seismic activity. The largest magnitude ever recorded corresponds to the 2007, m_{bLg} 5.1 Pedro Muñoz earthquake and the largest intensity ever reported is the V and corresponds to different events occurred in the province of Cuenca during the first part of the XX century (Garaballa 1919, Motilla del Palancar 1929). Accordingly, seismic hazard is low and current regulations do not enforce the development of any special plan for civil protection

against seismic risk.

However, there are tectonic structures with neotectonic activity in the area (Giner et al. 1996) with potential of generating a moderate event, as the faults bounding the Altomira Range (Figure 1).

Figure 1. Geologic map of the study area in Central Spain.

A limitation for ground motion characterization exists due to the limited availability of data on earthquake sources (e. g., focal mechanisms and fault slip rates) and of strong motion records. Therefore, synthetic ground-motion time histories are developed to model the ground shaking (both translation and rotation motions) at the wind turbine site.

3. SYNTHETIC GROUND MOTIONS

3.1. Ground Motion Definition

The seismic inputs used in this work (translational and rotational time histories) were theoretically generated for an earth layered structure embedding a double couple point source at shallow depths. The model takes into account the geometric and the inelastic attenuation of the medium (Q) for both P and S waves. Seismic events were characterized by a specific focal mechanism, moment magnitude and a Source-Time Function (STF) equivalent to an earthquake with circular finite rupture. The synthetic seismograms (accelerograms) were computed using the discrete wave-number method described by Bouchon and Aki (1977) and Bouchon (1979) for point dislocations. The velocity model assumed corresponds to the crustal properties of the south-eastern region of the Madrid Region, Spain (Corchete and Chourak, 2010; Table K).

Table 3.1. Crustal Structure used in this study

Layer	Z (m)	Vp (m/s)	Vs (m/s)	ρ (kg/m^3)	Qp	Qs
1	0	4380	2500	2280	200	100
2	1500	5430	3100	2280	200	100
3	5000	5600	3200	2740	200	100
4	10000	6480	3700	2740	200	100
5	15000	6650	3800	2800	400	200
6	30000	8050	4600	3050	400	200
7	40000	8230	4700	3050	400	200

The set of synthetic seismograms used here were generated for four different simulation groups (A, B, C and D) each of them with 30 different STF. Group A was simulated also for 30 different focal mechanisms randomly generated. Groups B, C and D were simulated using the mechanisms shown in table 3.2.

Table 3.2. Focal mechanisms for simulations B, C and D.

Group	Strike	Dip	Rale
B	180	75	175
C	135	75	175
D	259.1	22.1	51.9

The epicentre of the earthquake was located 23 km northeast of the wind turbine site. A Mw=5.5 earthquake at 6.5 km depth was assumed, which is the mean depth of seismicity in this region. The set of STF were randomly generated taking into account the mean properties of shallow crustal earthquakes of this magnitude (Tanioka and Ruff, 1997; Houston, 2001). STF were constructed assuming a lognormal shape (Liao y Huang, 2005), with skewness $0.15<S_k<0.35$ (Houston, 2001). They were added with 10% and 20% of white noise, low pass filtered at a f_c=25 hz and tapered at its extremes to avoid possible alias effects. The maximum total duration of these functions was τ=2.0s, with a mean duration of τ=1.5s at the 90% of the total moment release. Focal mechanisms were generated taking into account the tectonic setting of the region. In Figure 1 an example of two of the STF used in the study is shown.

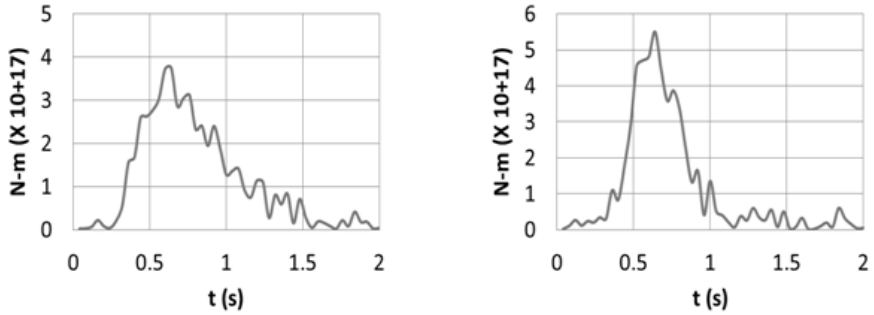

Figure 2. Source Time Functions for two of the simulated earthquakes.

Seismograms were synthesized in accelerations and displacements for each of the four groups and each STF simulation at four triaxial receivers located at the wind turbine placement. Seismograms were computed up to a frequency of 75.0 Hz and low pass filtered with a 4 pole Butterworth filter with a cut-off frequency of 40 Hz. From here the highest usable frequency is about 35.0 Hz. Once seismograms were generated, the time histories of rotations and angular accelerations were obtained by a first-order finite difference approach for the computation of the spatial derivatives of the ground motion.

Here, the complete tensor of synthetic displacement gradients $G_{i,j}=\Delta u_i/\Delta x_j$, where $\Delta u_{i,i}$=x,y,z, are the differences in the synthetic displacements in the three spatial directions and Δx_j , j=1,2,3 are the space increment in x, y and z directions respectively. The synthetic displacement time histories were computed again by the discrete wave-number method (Bouchon 1979). The spacing among computing points was taken as $\Delta x_j = \lambda_{min}/100=V_s/100\ f_N$, where $\Delta x_j=\Delta x_1=\Delta x_2=\Delta x_3$, V_s= minimum S wave velocity of the considered velocity structure, and f_N =maximum analyzed frequency. The time increment for this analysis $\Delta t=1/f_s=1/2f_N$. Once obtained the components of $G_{i,j}$, these were used to derive the rigid body rotations by:

$$\omega_{i,j} = \frac{1}{2}\left(\frac{\partial u_i}{\partial x_j} - \frac{\partial u_j}{\partial x_i} \right) \tag{5.1}$$

and the angular accelerations by:

$$\ddot{\omega}_{i,j} = \frac{\partial^2 \omega_{i,j}}{\partial t^2} \tag{5.2}$$

where i=1,2,3; j=1,2,3; u_1=u, u_2=v, u_3=w; u, v and w are the displacements in the x, y and z directions at a given time. At the surface, due to the stress free boundary conditions, three components of $G_{i,j}$ are not independent: $\partial u_1/\partial x_3 = -\partial u_3/\partial x_1$, $\partial u_2/\partial x_3 = -\partial u_3/\partial x_2$ and $\partial u_3/\partial x_3 = \eta\,(\partial u_2/\partial x_2 + \partial u_1/\partial x_1)$ and $\eta = -\lambda/(\lambda+2\mu)$; λ and μ are the Lamé parameters. From here, $\varepsilon_{1,3}=\varepsilon_{3,1}=\varepsilon_{2,3}=\varepsilon_{3,2}=0$. Cotton and Coutant (1997) tested this methodology with respect to the solution using analytic spatial derivatives, obtaining an excellent agreement with almost undistinguishable results between both techniques.

3.2. Sensitivity Analysis

A number of model parameters characterizing the fault, such as type of focal mechanism, source-time function and expected magnitudes are varied in order to study the sensitivity of the model to these input parameters.

All cases tested show that the predominant rotational component is around the Y axis, i. e., the axis connecting source and site locations (Figure 3).

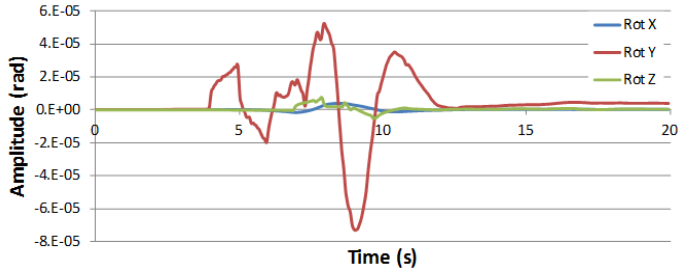

Figure 3. Rotational ground-motion time histories for a magnitude 6.0 event (source-to-site distance and depth are 20 and 7 km, respectively.

The rotational effect varies with magnitude and source-to-site distance. Rotation around Y axis for a magnitude 6.0 event is about one order of magnitude higher than for a magnitude 5.0 event. For relatively short distances (about 10 km), permanent rotation might be reached for moderate-high magnitude earthquakes (Figure 4).

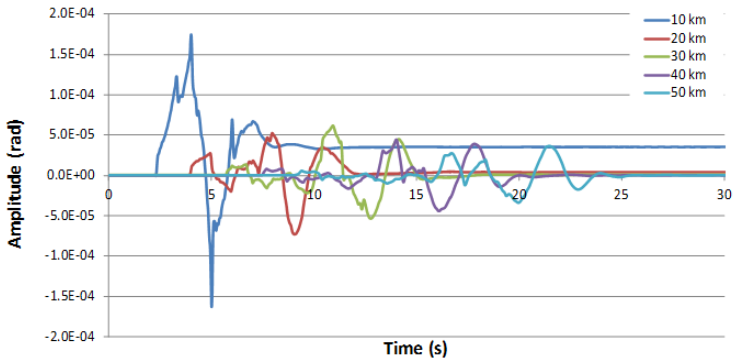

Figure 4. Rotational ground-motion time histories as a function of epicentral distance, for a magnitude 6.0 event and a depth of 7 km.

The impact of different focal mechanisms on modeled ground motions turned out to be significant and made it difficult to identify any variation pattern. Subsequent tests were made fixing the focal mechanism and varying source time functions, ensuring that the final STF was consistent with the

chosen magnitude of 5.5.

4. FINITE ELEMENT MODEL OF THE WIND TURBINE

Of course the simplest dynamical model has only 1 degree of freedom (dof). However, this type of model is not suited to represent adequately the dynamic response of a wind turbine during a seismic event. Much more sophisticated models that include several soil layers represent the opposite extreme leading to prohibitive calculation times. In the latter case 3d continuum elements are used for the soil, shell elements for the tower as well as the blades and concentrated masses to represent heavy equipment located in the nacelle. Fig. 5 presents some views of a wireframe model and a photograph.
A good compromise between accuracy and calculation times can be achieved by choosing a Finite Element (FE) model that represents a medium level of sophistication. To this end the soil's stiffness and damping properties are approximated by means of spring and damper elements that are located at the bottom of the footing. Apart from the spring and damper elements additional masses can also be included in order to account for the surrounding soil that accompanies the motion of the footing. The tower and the blades are modelled using beam elements. If the forces in the blades are not of special interest, rotor, nacelle and the heavy equipment may be modelled by means of concentrated masses at the top of the tower. The resulting FE model permits to study the contribution of the different bending modes to the overall response and allows studying the effects of changes in footing dimensions or soil properties. Therefore this type of model has been used for the simulations.

Figure 5. Wireframe model and photograph of the wind turbine MADE AE-46/1

As already mentioned in previous sections, the upper soil layer is very, very stiff. This should always be remembered when interpreting results presented in the present paper.

The highest excitation frequency is limited to approximately 30 Hz. With this in mind, a convergence study has been performed in order to end up with a suitable FE mesh. The varying diameter and thickness of the tower lead to continuously changing mass and stiffness properties between top and bottom. The used beam elements have a constant cross-section which increases the required number of elements. Finally, a mesh with 45 elements of equal length has been used for the simulations.

The characteristics of the fist eight modes of vibration are presented in table 4.1.

Table 4.2. Characteristics of the modes of vibration of the FE model.

Number	Type	Frequency (Hz)	Period (s)
1	Bending x direction	0.7910	1.264
2	Bending z direction	0.7910	1.264
3	Bending x direction	6.7766	0.148
4	Bending z direction	6.7766	0.148
5	Axial transl. y dirct.	16.8137	0.059
6	Bending x direction	19.8609	0.050
7	Bending z direction	19.8609	0.050
8	Torsion rot y	26.4675	0.038

Rayleigh damping equivalent to 1 % of critical damping has been used using the frequencies of the first and third modes.

5. RESULTS

5.1. Results considering the first set of ground motions

A total of 60 simulations have been carried out, two for each of the 30 sets of time history accelerations: once considering that the ground motion produces only motion on the translational dof at the base, and a second one with additional motion on the rotational dof.

For a given seismic input, the results with or without rotational seismic input may be very similar. Comparisons may be established in terms of the maximum value of Von Mises stresses at a given section of the tower. Fig.6 (a) shows this magnitude as a function of the height of the tower considering both kinds of seismic input for a given set of time history accelerations. In this case differences are smaller than 10%. Fig. 6 (b) displays the same plot for a different set. This time differences are much more important, indicating that for this set the base rotations do have a big influence on the response of the tower.

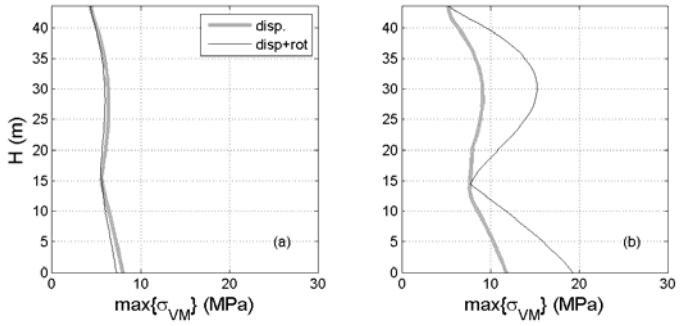

Figure 6. Comparison of the distribution of maximum Von Mises stress along the tower's height with or without rotational input for records: (a) no.12 and (b) no.18.

The observed differences between responses caused by both records can be easily explained by the means of response spectra. They are displayed in figure 7 for horizontal ground motions and rotations around the horizontal axis. The differences in the radiation pattern between both cases as well as resonance effects between vibration frequencies of the top soil layer and main structural modes may explain the discrepancies.

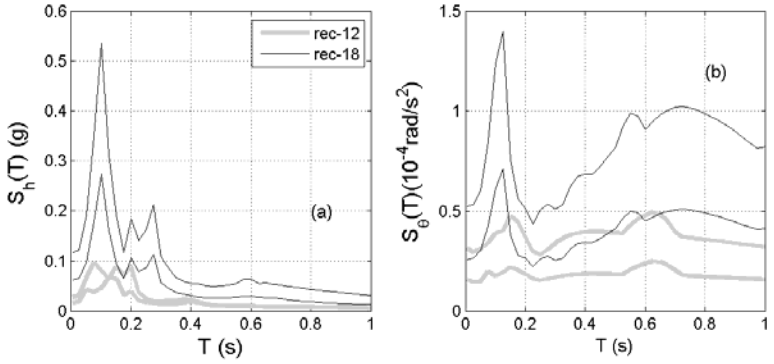

Figure 7. Comparison of the distribution of maximum Von Mises stress along the tower's height with or without rotational input for records: (a) no.12 and (b) no.18.

In order to assess the differences obtained between simulations with or without the rotational seismic input, results from all simulations have been analyzed globally. For each section (height) the maximum value of the Von Mises stress resulting from each simulation has been considered as a realization of a random variable X. It has been assumed that X distributes as a lognormal random variable, and its two parameters have been estimated from the 30 samples available. Fig. 8 shows plots of the probability density functions for both cases at three different heights. At the base (0m) and around 30m both distributions are quite different. However this is not the case at 15m. The reason is that that modes number 3 and 4, which are the ones that are excited significantly by base rotations, have reduced moments at this height

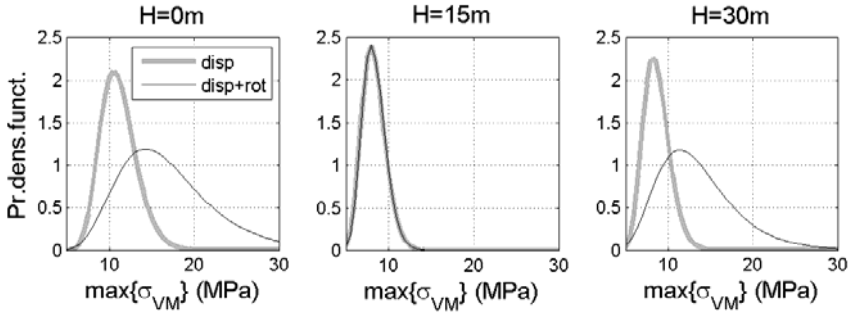

Figure 8. Comparison of probability density functions of maximum Von Mises stress at sections placed at different heights of the tower.

The obtained values indicate that there is a large scatter among results. Some records display important differences while others do not fit this point. It is not clear whether important differences are associated to particular focal mechanism or to particular SF. This question is addressed next.

5.2. Results considering sets B, C and D

For each record of the new sets, again two simulations have been done: one considering the rotational seismic components, and another without them. The importance of the rotational components will be assessed using the following ratio

$$\frac{\max\left(\sigma_{VM,disp+rot}\right)}{\max\left(\sigma_{VM,disp}\right)}. \tag{5.3}$$

High values of the ratio indicate that rotations are important, while values close to unity indicate the opposite.

Figure 9 displays the cumulative distribution function (CDF) of the ratios for the three sets. Set C has an almost vertical CDF indicating that all the ratios are close to 1. Discrepancies between results with or without rotational components are noticeable for the records in set B, and remarkably important for those in set D.

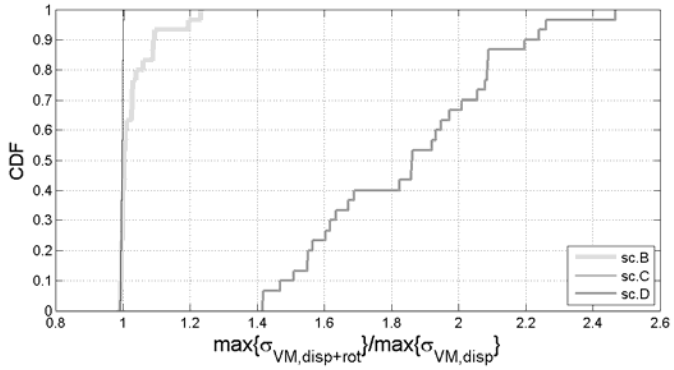

Figure 9. Comparison of cumulative distribution functions or the ratio between the maximum Von Mises stresses obtained with and without rotational seismic components.

6. CONCLUSIONS

The analysis of synthetic time histories of translational and rotational motions indicates the significant effect of the rotational components of motion, especially for short distances and moderate magnitudes.

The results obtained in this study indicate the importance of the rotational components of ground motions on wind turbine response patterns.

The importance of the rotational components is directly related to its magnitude, which is highly dependent on the focal mechanisms. Source time functions have proven to also have an effect on it, but it only arises with suitable focal mechanisms.

AKCNOWLEDGEMENT

The work presented in this paper is partly funded by the Universidad Politécnica de Madrid and by the Comunidad Autónoma de Madrid.

REFERENCES

Bouchon, M. and K. Aki (1977). Discrete wave-number representation of seismic-source wave fields. Bulletin of the Seismological Society of America **67:2**,259-277.

Bouchon, M. (1979), discrete wavenumber representation of elastic wave fields in three-space dimensions, Journal of Geophysical Research **84**, 3609–3614.

Cotton F., Coutant O. (1997) Dynamic stress variations due to shear faults in a plane-layered medium. Geophys. J. Int.,128,676-688.

Corchete V. and M. Chourak (2011). Shear-wave velocity structure of the south-eastern part of the Iberian Peninsula from Rayleigh wave analysis. International Journal of Earth Sciences, **100**, 1733-1747.

Giner, J. L., G. De Vicente, A. C. Pérez González, J. G. Sánchez Cabañero, and L. Pinilla (1996). Crisis tectónicas cuaternarias en la Cuenca de Madrid. Geogaceta **20:4**, 842–845.

Houston, H. (2001). Influence of depth, focal mechanism, and tectonic setting on the shape and duration of earthquake source time functions. Journal of Geophysical Research **106:b6**, 11,137-11,150.

Liao B. Y. and Huang H.C. (2005). Estimation of the source time function based on blind deconvolution with Gaussian mixtures. Pure Appl. Geophys. PAGEOPH 162, 479–494. 16 doi 10.1007/s00024-004-2617-z; 0033 – 4553/05/030479.

Tanioka, Y. and L. J. Ruff (1997) Source Time Functions. Seismological Research Letters **68:3**, 386-400.